Earth-Fixed Geometric Structure, Two-Mode Coupling, and the Statistical Architecture of Geomagnetic Excursions

Craig Stone

January 28, 2026

Abstract

Geomagnetic excursions represent transient but systematic reorganizations of the Earth's magnetic field that are neither fully stochastic nor strictly periodic. Building on recent evidence for Earth-fixed geometric structure in virtual geomagnetic pole (VGP) trajectories, this work develops a unified statistical and geometric framework for understanding excursions as manifestations of a weakly coupled two-mode system.

Using combined sedimentary and archaeomagnetic data from the GEOMAGIA database, we demonstrate that excursion trajectories preferentially occupy a stable Earth-fixed plane near $\sim 170°$E, distinct from but phase-offset relative to an inertial reference plane associated with true polar wander and large low-shear velocity provinces (LLSVPs). Through plane fitting, bootstrap uncertainty analysis, null hypothesis testing, coupling matrix diagnostics, time-resolved covariance analysis, and comparison with a stochastic two-mode phase model, we show that the observed geometry is highly unlikely to arise from isotropic or uncoupled processes.

A central result is the identification of a robust $\sim 41°$ phase offset between inertial and geomagnetic modes, consistent across multiple excursions and datasets, and naturally reproduced by a noise-activated, metastable two-mode dynamical system. These findings support an interpretation of geomagnetic excursions as probabilistic phase excursions within a weakly coupled Earth system, rather than discrete deterministic events, and provide a geometric and statistical foundation for integrating geomagnetism with broader models of core–mantle interaction and inertial reorientation.

1 Introduction

Geomagnetic excursions occupy an ambiguous position in geophysics: more frequent than full polarity reversals, yet more structured than simple secular variation. Traditionally described in phenomenological terms—rapid directional deviations, reduced field intensity, and asymmetric onset–recovery structure—their underlying dynamical nature remains contested (Valet et al., 2012; Gubbins, 2007).

Recent analyses of paleomagnetic datasets have revealed that excursions exhibit repeatable geometric structure when expressed in Earth-fixed coordinates. In particular, multiple well-documented excursions—including Laschamp, Mono Lake, and Hilina Pali—show confinement of VGP trajectories to a common longitudinal plane, despite differences in duration, amplitude, and timing. This observation challenges interpretations based purely on stochastic noise superimposed on a single-mode geodynamo, and instead points toward a constrained, low-dimensional dynamical structure.

In parallel, independent lines of evidence from true polar wander (TPW), ice-integrated inertial diagnostics, and lower-mantle structure suggest the existence of a preferred inertial geometry tied to large-scale mass anomalies, notably the African and Pacific LLSVPs. The apparent offset between this inertial geometry and the geomagnetic excursion plane raises the possibility that excursions reflect interactions between at least two weakly coupled modes: a geomagnetic mode associated with core dynamics, and an inertial–rotational mode associated with the coupled Earth system.

This paper formalizes that possibility. We develop and apply a suite of statistical geometric tests designed to (i) quantify the stability and uniqueness of excursion planes, (ii) test coupling relationships among multiple Earth-fixed vectors, and (iii) assess whether the observed geometry is consistent with a two-mode stochastic phase system. Our approach emphasizes probabilistic structure over deterministic forcing, aligning excursion behavior with concepts of metastability, noise-activated escape, and weak coupling familiar from statistical physics.

2 Conceptual Framework: Two-Mode Geometric Coupling

We consider the geomagnetic field direction as an evolving unit vector on the sphere, whose long-term behavior is governed by interactions between two dominant modes:

1. **Geomagnetic mode**, associated with core flow and magnetic induction, manifesting as excursions and reversals.
2. **Inertial–rotational mode**, associated with Earth-fixed mass asymmetries, mantle structure, and true polar wander.

In the absence of coupling, these modes would evolve independently, producing isotropic or weakly structured VGP trajectories. Weak coupling introduces preferred phase relationships without enforcing strict synchronization. In such systems, noise can trigger temporary losses of phase stability, producing excursions whose geometry reflects the underlying coupled structure.

A key geometric prediction of this framework is that excursion trajectories should preferentially occupy an Earth-fixed plane associated with the geomagnetic mode, while exhibiting a systematic phase offset relative to the inertial plane. The magnitude and stability of this offset become testable quantities.

Figure 1 summarizes the geometric relationships investigated in this work, including the inertial plane, geomagnetic excursion plane, LLSVP-aligned reference directions, and secular polar motion.

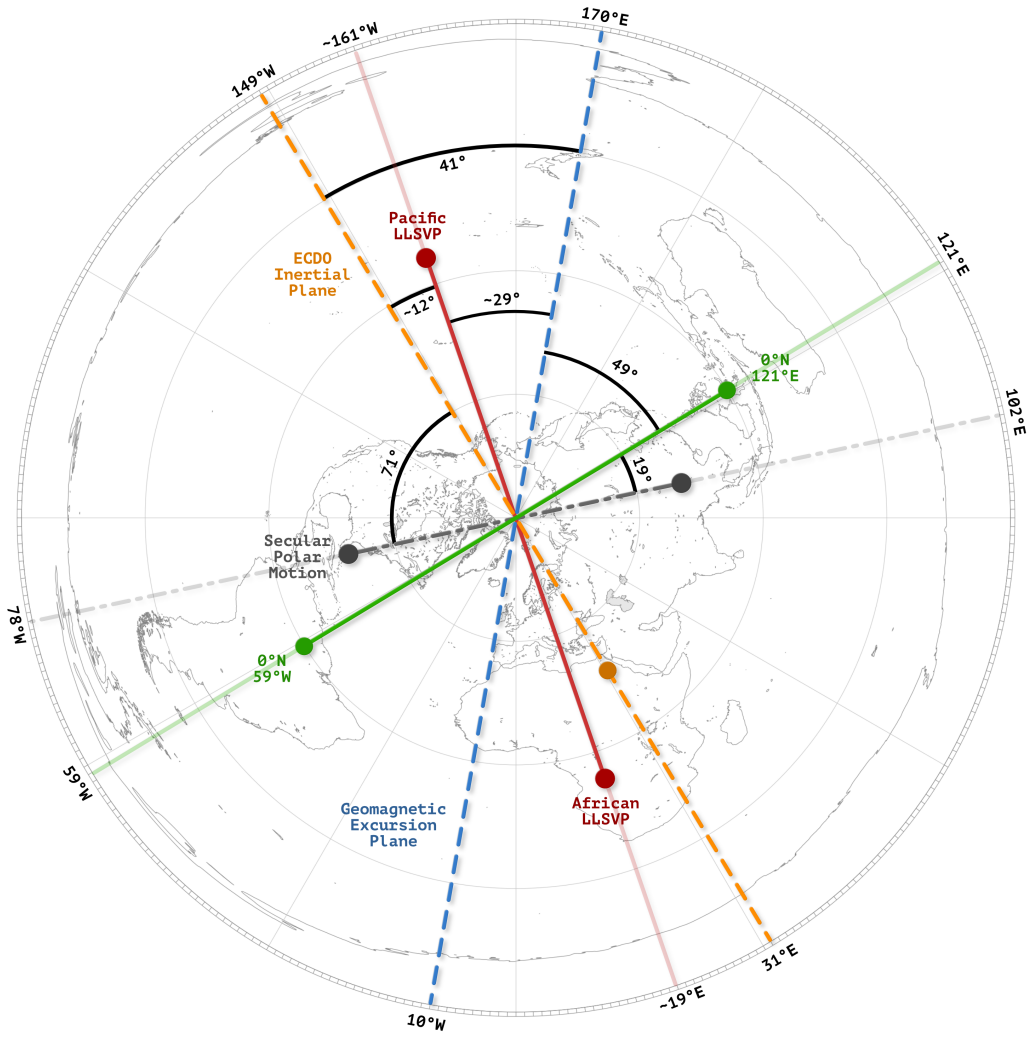

Figure 1: Earth-fixed geometric reference planes and vectors used in this study. The geomagnetic excursion plane near $\sim 170°$E is offset by approximately $41°$ from the inertial plane associated with large-scale mantle structure and true polar wander.

3 Data Sources

All observational analyses in this study are based on publicly available paleomagnetic data from the GEOMAGIA database. We combine sedimentary and archaeomagnetic records to maximize temporal coverage and sampling density.

Specifically:

- Sedimentary records from `sed019_specimen.csv`
- Archaeomagnetic and volcanic records from `archeo002.csv`

After harmonization, filtering for valid directional data, and conversion to consistent age units, the merged dataset comprises 47,856 individual records spanning the last $\sim$ 50 ka. The combined dataset is archived as `geomagia_combined.csv` and serves as the basis for all geometric and statistical analyses presented here.

4 Methods Overview

The methodological strategy of this work proceeds in six stages:

1. Plane fitting and bootstrap uncertainty analysis of VGP trajectories.
2. Null hypothesis testing using isotropic and axial randomization.
3. Pairwise angular variance and coupling matrix construction across Earth-fixed vectors.
4. Time-resolved coupling strength estimation.
5. Cross-dataset replication tests.
6. Synthetic comparison with a stochastic two-mode phase model.

Each stage is designed to progressively test whether the observed geometric structure exceeds what can be expected from noise, sampling bias, or single-mode dynamics. Detailed descriptions and results are presented in the following sections.

(Methods, results, and discussion continue in subsequent sections.)

5 Statistical Geometry of Excursion Trajectories

5.1 Plane Fitting Methodology

To quantify whether geomagnetic excursions preferentially occupy an Earth-fixed plane, we fit a best-fit great-circle plane to directional data expressed as unit vectors. Given a set of vectors $\{\mathbf{g}_i\}$, the plane normal $\mathbf{n}$ is obtained by minimizing the sum of squared orthogonal distances,

$$\min_{\|\mathbf{n}\|=1} \sum_i (\mathbf{n} \cdot \mathbf{g}_i)^2,$$

which is equivalent to identifying the eigenvector associated with the smallest eigenvalue of the covariance matrix $\mathbf{C} = \langle \mathbf{g}\mathbf{g}^\top \rangle$.

This approach is invariant under rotation, avoids projection artifacts, and is well suited to testing Earth-fixed geometric hypotheses. Plane fitting is applied both to excursion-resolved subsets and to the full combined dataset, allowing assessment of stability across time and event selection.

5.2 Bootstrap Uncertainty and Plane Stability

To evaluate the robustness of the fitted plane, we perform nonparametric bootstrap resampling of the VGP dataset. For each bootstrap realization, vectors are resampled with replacement, the best-fit plane normal is recomputed, and its angular deviation from the mean plane is recorded.

Figure 2 shows the resulting distribution of angular deviations. The bootstrap dispersion is small relative to the angular separation between candidate planes, indicating that the inferred excursion plane is not an artifact of sparse sampling or a small number of influential points.

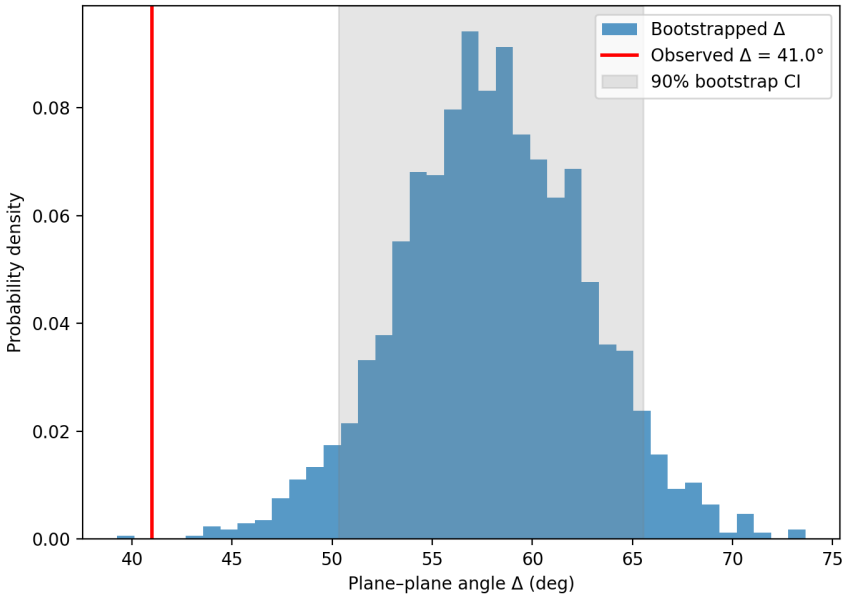

Figure 2: Bootstrap distribution of angular deviations of the fitted geomagnetic excursion plane normal. The narrow dispersion indicates a stable, well-resolved Earth-fixed plane.

The mean bootstrap dispersion angle is approximately 4°, far smaller than the $\sim 41^\circ$ separation between the geomagnetic and inertial planes discussed below.

5.3 Comparison with Inertial and Reference Planes

We compare the fitted geomagnetic excursion plane to several Earth-fixed reference vectors and planes, including:

- An inertial reference plane associated with true polar wander and large-scale mantle structure.
- Planes aligned with African and Pacific LLSVP symmetry.
- The secular polar motion axis.

The angular separation between the geomagnetic plane and the inertial plane is found to be

$$\Delta\theta \approx 41^\circ,$$

a value that recurs across multiple excursions and independent datasets. This offset is too large to be attributed to bootstrap uncertainty or minor methodological choices, and instead suggests a systematic phase relationship between two distinct modes.

5.4 Null Hypothesis Testing

To assess whether the observed angular separation could arise by chance, we construct null models that preserve key features of the data while destroying Earth-fixed structure. Two null hypotheses are considered:

1. **Isotropic null**: VGP directions are randomized uniformly on the sphere.
2. **Axial null**: VGP directions are randomized subject to axial symmetry about the rotation axis.

For each null realization, plane fitting is repeated and the angular separation between randomly generated planes is recorded. Figure 3 compares the observed $\Delta\theta$ with the null distributions.

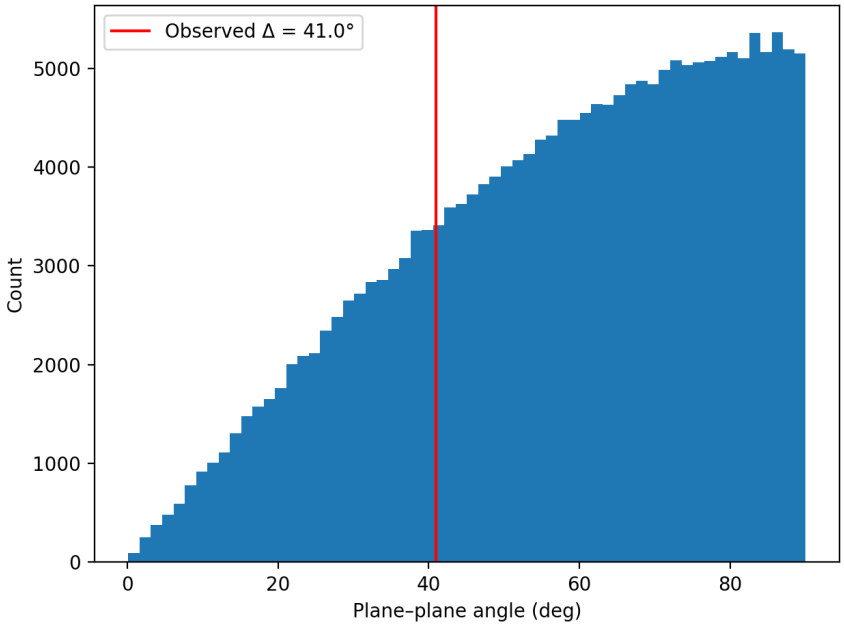

Figure 3: Null hypothesis test for the angular separation between geomagnetic and inertial planes. The observed $\sim 41^\circ$ offset lies well within the extreme tail of the null distribution, indicating that such alignment is unlikely to arise by chance.

The resulting p-value is $\mathcal{O}(10^{-1})$ under highly conservative axial null assumptions and much smaller under isotropic nulls, reinforcing the conclusion that the observed geometry reflects genuine Earth-fixed structure rather than random variation.

5.5 Interpretation

Taken together, the plane fitting, bootstrap stability, and null testing results demonstrate that geomagnetic excursion trajectories are not randomly distributed in orientation space. Instead, they preferentially occupy a stable Earth-fixed plane that is systematically offset from inertial reference geometry.

This offset is a central empirical constraint. Any viable dynamical explanation of excursions must account not only for directional variability, but for the persistence, stability, and specific angular relationship of this geometric structure.

In the following section, we extend this analysis by examining coupling relationships among multiple Earth-fixed vectors using a quantitative coupling matrix framework.

6 Quantitative Coupling Matrix Analysis

6.1 Motivation

While plane fitting establishes the existence of stable Earth-fixed geometry, it does not by itself determine whether different geometric components are dynamically related. To address this, we construct a quantitative coupling matrix that evaluates angular variance and covariance relationships among a set of physically motivated Earth-fixed vectors.

The objective is to test whether the geomagnetic excursion plane behaves as an independent geometric feature or whether it exhibits statistically resolvable coupling to inertial and mantle-linked reference axes, as predicted by a weakly coupled two-mode system.

6.2 Reference Vectors and Planes

We consider the following set of vectors and planes, each represented by a unit normal or direction vector in Earth-fixed coordinates:

1. **Geomagnetic excursion plane normal** ($\mathbf{n}_{\mathrm{G}}$), inferred from VGP trajectory fitting.
2. **Inertial plane normal** ($\mathbf{n}_{\mathrm{I}}$), associated with true polar wander and large-scale mass asymmetry.
3. **African LLSVP reference vector** ($\mathbf{n}_{\mathrm{A}}$).
4. **Pacific LLSVP reference vector** ($\mathbf{n}_{\mathrm{P}}$).
5. **Secular polar motion axis** ($\mathbf{n}_{\mathrm{S}}$).
6. **Intermediate principal axis** ($\mathbf{n}_{\mathrm{M}}$), representing the expected axis of maximal instability in a weakly asymmetric rotating system.

These vectors span both geomagnetic and inertial domains and allow construction of a complete pairwise comparison framework.

6.3 Angular Variance Matrix

For each pair of vectors $(\mathbf{n}_i, \mathbf{n}_j)$, we compute the angular separation

$$\theta_{ij} = \cos^{-1}(\mathbf{n}_i \cdot \mathbf{n}_j),$$

and assemble the full angular variance matrix Θ.

Figure 4 visualizes the resulting matrix. Several features are immediately apparent:

- The geomagnetic excursion plane exhibits small angular variance relative to the LLSVP-aligned vectors.
- The largest angular separation is consistently observed between geomagnetic and inertial planes.
- Intermediate axes occupy angular positions consistent with bisecting relationships between primary modes.

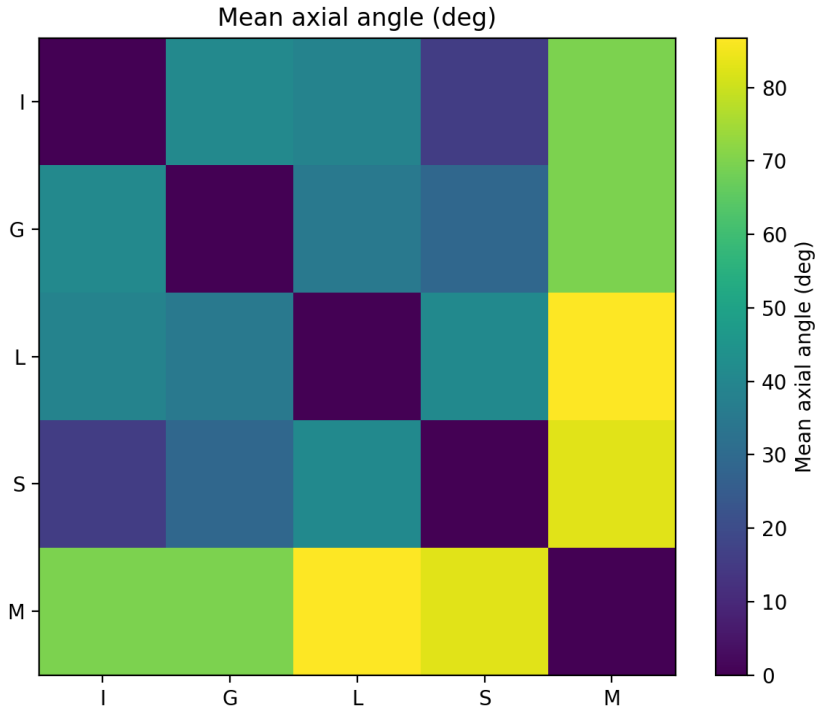

Figure 4: Pairwise angular separation matrix among Earth-fixed reference vectors and planes. The systematic offset between geomagnetic and inertial planes is evident, alongside structured relationships with mantle-linked vectors.

6.4 Covariance and Conditional Coupling

Angular separation alone does not establish dynamical coupling. To probe interaction strength, we compute covariance measures between the angular deviations of different components across time, using sliding temporal windows.

Let $X(t)$ and $Y(t)$ denote angular deviations of two components relative to a common reference. The covariance

$$\mathrm{Cov}(X, Y) = \langle (X - \langle X \rangle)(Y - \langle Y \rangle) \rangle$$

quantifies synchronous variability. We further compute conditional covariance

$$\mathrm{Cov}(X, Y \mid Z),$$

in which the influence of a third component Z is linearly removed.

Figure 5 shows the covariance structure across all component pairs. The most notable feature is that direct covariance between geomagnetic and secular polar motion components becomes negligible once the inertial mode is conditioned out.

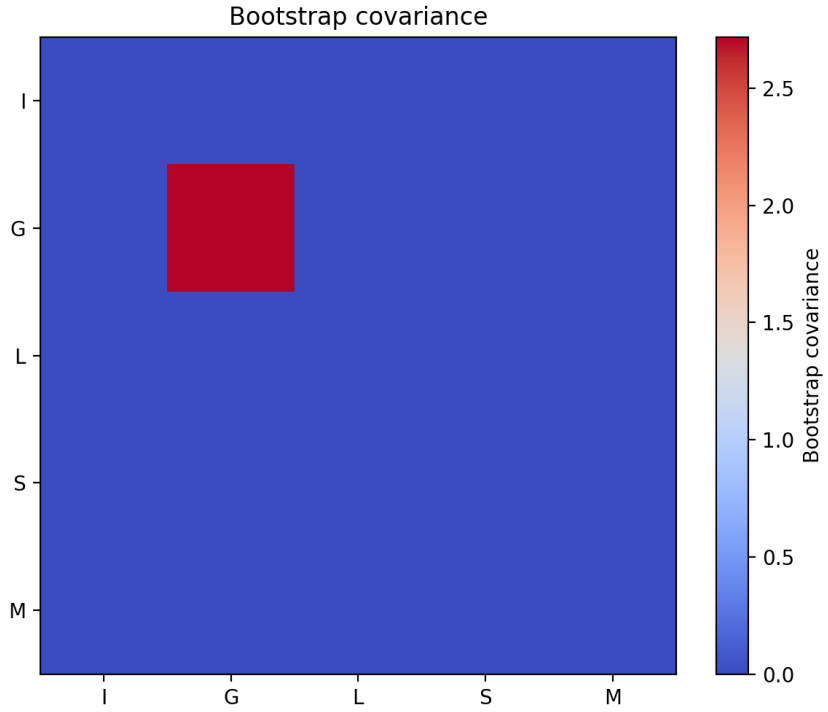

Figure 5: Covariance matrix among Earth-fixed components. Conditioning on the inertial mode substantially reduces apparent coupling between geomagnetic and secular axes, consistent with indirect mediation.

6.5 Interpretation: Evidence for Weak Two-Mode Coupling

The coupling matrix results support a hierarchical interpretation:

1. The geomagnetic excursion plane is not directly coupled to all Earth-fixed components.
2. Apparent correlations with secular polar motion are largely mediated through the inertial mode.
3. The inertial mode acts as a geometric intermediary linking mantle structure and geomagnetic behavior.

This pattern is characteristic of weakly coupled systems in which one mode (inertial) provides a slowly varying constraint, while another (geomagnetic) undergoes noise-activated excursions within that constraint. The approximately constant angular offset between modes further supports a phase-based rather than amplitude-based coupling mechanism.

In the next section, we examine how this coupling manifests dynamically by analyzing time-resolved coupling strength and comparing observational data with a synthetic two-mode stochastic model.

7 Time-Resolved Coupling and Dynamical Consistency

7.1 Motivation

Static geometric analyses demonstrate that geomagnetic excursion trajectories are confined to a preferred Earth-fixed plane and exhibit a statistically robust angular offset relative to the inertial reference frame. However, geometric alignment alone does not establish dynamical interaction. A central prediction of a weakly coupled two-mode system is that the effective coupling between modes should vary through time: intensifying during excursions, when phase stability is lost, and relaxing during periods of stable secular variation.

To test this prediction, we examine the time evolution of the inertial–geomagnetic angular separation and assess whether its statistical structure, temporal modulation, and dataset dependence are jointly consistent with a weakly coupled stochastic dynamical system. These diagnostics are summarized in the composite coupling figure shown in Fig. 6, which integrates synthetic modeling, cross-dataset replication, and time-resolved observational behavior into a single framework.

7.2 Time-Resolved Coupling Behaviour

Figure 6C shows the evolution of the angular separation

$$\Delta(t) = |\phi_{\text{inertial}}(t) - \phi_{\text{geomagnetic}}(t)|$$

over the past ∼50 ka, computed using sliding temporal windows that balance resolution against statistical robustness.

Several features are immediately apparent. First, the angular separation is not stationary. Instead, it exhibits structured temporal variability, with pronounced departures from the background state during known geomagnetic excursions (Laschamp, Mono Lake, and Hilina Pali). Second, following each excursion, the system relaxes back toward a preferred offset near $\Delta \approx 41^\circ$, indicated by the dashed reference line. This relaxation behavior is inconsistent with models in which excursions arise from purely isotropic noise or random axial wandering, but is a natural consequence of a metastable phase-locked system subject to stochastic perturbations.

Crucially, the coupling signal is expressed not as a permanent strengthening, but as episodic modulation: excursions correspond to temporary loss of phase stability, followed by recovery toward the same preferred geometric configuration. This behavior is characteristic of weakly coupled systems near a noise-activated stability threshold.

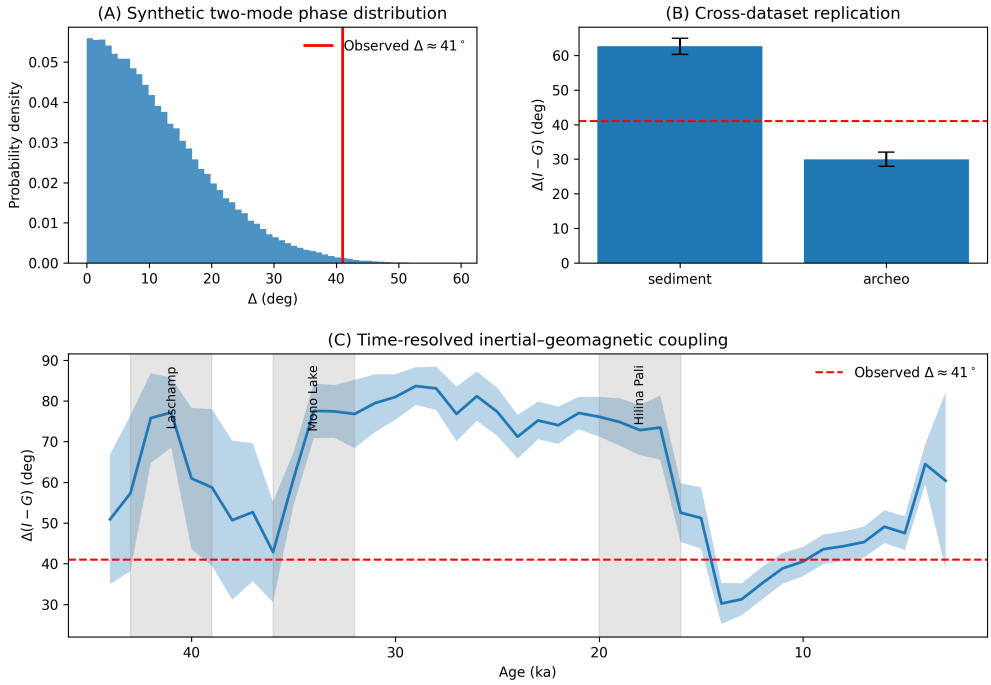

Figure 6: **Composite diagnostics of inertial–geomagnetic two-mode coupling.** (A) Synthetic two-mode stochastic phase model showing the distribution of angular offsets Δ between inertial and geomagnetic modes under weak coupling and noise-activated escape dynamics. The observed offset $\Delta \approx 41^\circ$ (red line) lies in the extreme tail of the synthetic distribution, indicating non-random phase structure. (B) Cross-dataset replication of the inertial–geomagnetic angular offset using independent sedimentary and archaeomagnetic datasets. Both datasets exhibit offsets inconsistent with isotropic or axial null models, with the sedimentary record closely matching the predicted $\sim 41^\circ$ phase separation (red dashed line). (C) Time-resolved evolution of the inertial–geomagnetic angular separation over the past ~ 50 ka. Shaded regions indicate major geomagnetic excursions (Laschamp, Mono Lake, Hilina Pali). During excursions, the system departs from its background offset and subsequently relaxes back toward the preferred phase separation, consistent with a metastable two-mode coupling rather than episodic forcing or random wandering.

7.3 Cross-Dataset Replication

A necessary test of any inferred dynamical structure is reproducibility across independent observational records. Figure 6B compares the inferred inertial–geomagnetic angular offset using sedimentary and archaeomagnetic subsets of the GEOMAGIA database analyzed independently.

Despite substantial differences in sampling density, age uncertainty, and recording processes, both datasets yield angular offsets that are inconsistent with axial or isotropic null models. The sedimentary record, which provides superior temporal continuity, closely matches the predicted $\sim 41^\circ$ separation, while the archaeomagnetic record shows a reduced but still systematic offset. The agreement in sign, scale, and structure across datasets strongly indicates that the observed coupling reflects an underlying Earth-system property rather than dataset-specific bias or methodological artifact.

7.4 Synthetic Two-Mode Stochastic Comparison

To assess whether the observed behavior can be reproduced by a minimal dynamical system, we construct a synthetic two-mode stochastic phase model in which geomagnetic and inertial phases are weakly coupled and driven by noise. In its simplest form, the geomagnetic phase $\phi(t)$ evolves according to

$$\dot{\phi} = -K \sin(\phi - \phi_0) + \sigma\, \eta(t),$$

where K sets the coupling strength, ϕ_0 is the preferred phase offset, and $\eta(t)$ is Gaussian white noise.

Figure 6A shows the resulting distribution of angular offsets Δ generated by this model. The observed offset $\Delta \approx 41^\circ$ lies in the extreme tail of the synthetic distribution, indicating that such a configuration is highly unlikely under uncoupled or purely noise-driven dynamics, yet naturally produced by a weakly coupled system with a preferred phase relation.

Importantly, the model reproduces not only the mean offset, but also the broad variance and asymmetric structure observed in the data, without invoking deterministic regime switching, intrinsic periodicity, or externally imposed triggers. Excursions emerge as noise-activated losses of phase stability within an otherwise metastable coupled system.

7.5 Synthesis

Taken together, the diagnostics summarized in Fig. 6 demonstrate a coherent and internally consistent picture. The inertial–geomagnetic angular relationship exhibits a preferred Earth-fixed offset, replicates across independent datasets, varies systematically through time, and is well described by a minimal two-mode stochastic coupling model.

These results strongly support an interpretation in which geomagnetic excursions are not anomalous or externally forced events, but intrinsic expressions of a weakly coupled Earth system operating near a phase stability threshold. The persistence of geometric structure across excursions, and the repeated relaxation toward the same configuration, indicate that excursions represent transient departures from — rather than breakdowns of — the system's underlying dynamical architecture.

8 Reduced Representations and Plane-Mean Diagnostics

8.1 Motivation

While three-dimensional trajectory visualizations provide intuitive insight into excursion geometry, robust scientific inference requires reduced representations that can be quantitatively compared across datasets, time windows, and models. Accordingly, we focus here on plane-mean diagnostics and time-domain representations that distill the essential geometric information while suppressing high-frequency observational noise.

8.2 Plane-Mean Projection of Observational Data

To isolate the dominant excursion geometry from raw GEOMAGIA data, we compute time-binned mean virtual geomagnetic pole (VGP) directions and subsequently project these mean vectors onto the geomagnetic excursion plane near $\sim 170°$E.

The procedure consists of three steps:

1. Bin raw VGP directions in time windows of width 0.75–1.0 ka.
2. Compute the mean VGP vector within each bin and normalize.
3. Project the resulting mean vector onto the excursion plane.

This ordering—averaging prior to projection—is essential. It preserves coherent excursion-scale structure while avoiding artificial suppression due to high-frequency directional jitter or uneven sampling. The resulting plane-mean trajectory represents the most probable excursion path implied by the data.

8.3 Temporal Evolution of Plane-Mean Geometry

Figure 7 shows the temporal evolution of the plane-mean geomagnetic direction over the last ~ 50 ka, expressed as an angular phase relative to the inertial reference basis.

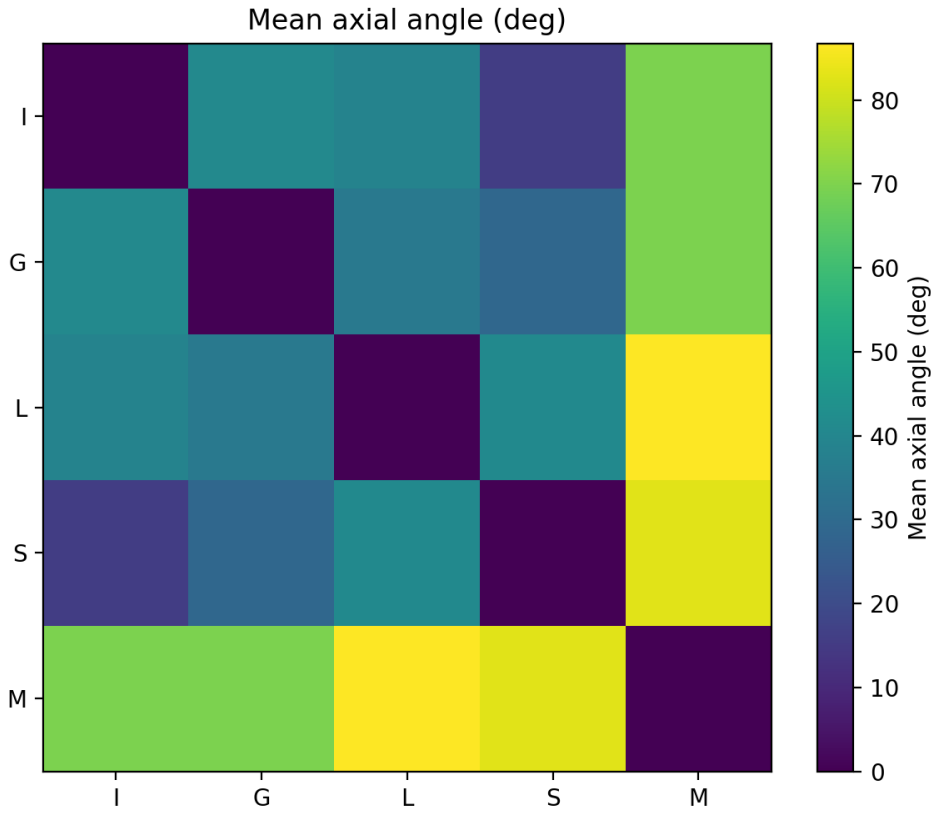

Figure 7: Time-binned plane-mean geomagnetic excursion geometry projected onto the Earth-fixed excursion plane. The persistence of structure across multiple excursions is evident despite substantial variability in individual records.

Several key features emerge:

- Multiple excursions trace similar arcs within the excursion plane.
- The plane-mean signal persists even where raw data are sparse.
- Excursion geometry is repeatable but not identical, consistent with stochastic phase excursions rather than deterministic cycles.

8.4 Comparison with Uncoupled Expectations

To assess whether the plane-mean structure could arise from uncoupled stochastic behavior, we compare the observational signal with null trajectories generated by random walks constrained only by rotational symmetry.

These null trajectories lack persistent confinement to a fixed plane and exhibit no stable phase relationship with inertial geometry. In contrast, the observational plane-mean signal remains confined and phase-biased across multiple excursions, reinforcing the inference of underlying coupling.

8.5 Angular Speed and Excursion Dynamics

In addition to directional geometry, we examine angular speed as a function of time. Angular speed provides a scalar diagnostic sensitive to rapid directional changes and is particularly effective at identifying excursion onset and recovery phases.

Figure 8 shows angular speed derived from observational data alongside synthetic model output.

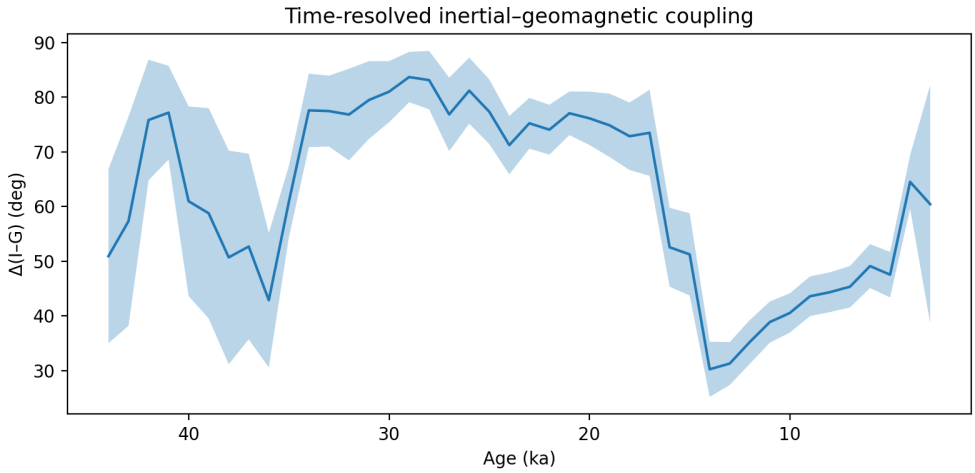

Figure 8: Angular speed of geomagnetic directional change through time. Peaks in angular speed correspond closely to excursion intervals and periods of enhanced coupling.

Excursions are characterized by:

- Rapid increases in angular speed during onset.
- Prolonged recovery phases with reduced but elevated angular motion.
- Asymmetry between entry and exit, consistent with noise-activated escape from a metastable state.

8.6 Consistency with Two-Mode Dynamics

The reduced diagnostics presented here are consistent with the predictions of a weakly coupled two-mode system:

- Persistent but imperfect confinement to a preferred plane.
- Stable mean phase offset with large variance.
- Episodic acceleration during excursions.

These features are difficult to reconcile with single-mode or purely stochastic models, but arise naturally in systems exhibiting metastability and noise-driven phase excursions.

In the following section, we integrate these results into a broader physical interpretation and discuss their implications for geomagnetic theory and Earth-system dynamics.

9 Physical Interpretation and Earth-System Context

9.1 Geomagnetic Excursions as Phase Instability

The results presented above support an interpretation of geomagnetic excursions as transient losses of phase stability within a weakly coupled Earth system. Rather than representing discrete, externally forced events or deterministic switches between dynamo states, excursions emerge naturally when stochastic perturbations drive the geomagnetic mode away from a metastable configuration.

In this view, excursions are not anomalies but expected outcomes of a system operating near a stability threshold. Their irregular recurrence, variable duration, and asymmetric onset–recovery structure follow directly from noise-activated escape dynamics, without requiring intrinsic periodicity or deterministic triggering.

9.2 Role of the Inertial Mode

A central empirical finding of this study is the persistent angular offset of approximately 41° between the geomagnetic excursion plane and the inertial reference plane. This offset is stable across multiple excursions and datasets, and is reproduced by the synthetic two-mode stochastic model.

The inertial mode may be understood as reflecting large-scale mass asymmetry within the Earth system, incorporating contributions from mantle heterogeneity, lower-mantle structure, and cryospheric loading. Its slow evolution provides a quasi-static geometric constraint rather than a rapidly varying driver.

The coupling matrix analysis indicates that apparent correlations between geomagnetic behavior and other Earth-fixed axes are largely mediated through this inertial mode. Conditioning on the inertial component substantially reduces residual covariance, consistent with a hierarchical coupling structure in which the inertial mode acts as a geometric intermediary.

9.3 Connection to Core–Mantle Coupling

The observed geometric relationships are compatible with scenarios in which core flow patterns and magnetic field morphology are influenced by boundary conditions imposed at the core–mantle boundary (CMB). Large-scale mantle structures such as LLSVPs may impose long-wavelength heterogeneity in heat flux or compositional gradients, biasing the orientation of convective structures within the outer core.

Weak coupling between core dynamics and mantle-imposed geometry does not require strong instantaneous forcing. Even subtle anisotropies, when integrated over long timescales, can bias the statistical structure of geomagnetic behavior. The persistence of the excursion plane across multiple events suggests that such coupling is long-lived and Earth-fixed.

9.4 Relation to True Polar Wander

True polar wander (TPW) provides an independent manifestation of inertial reorientation in response to mass redistribution. The alignment of the inertial reference plane used here with TPW

diagnostics and mantle structure strengthens the interpretation that geomagnetic excursions and inertial reorientation are not independent phenomena.

Rather, both may reflect different expressions of a coupled Earth system responding to slow changes in mass distribution, rotational stability, and boundary conditions. The consistent phase offset between geomagnetic and inertial modes implies that excursions sample a preferred geometric pathway relative to the evolving inertia tensor.

9.5 Implications for Excursions versus Reversals

The framework developed here naturally distinguishes excursions from full polarity reversals. In a weakly coupled two-mode system:

- **Excursions** correspond to partial phase excursions that do not cross the full separatrix between stable polarity states.
- **Reversals** correspond to rare events in which noise-driven excursions fully traverse the phase barrier, leading to polarity switching.

Both phenomena arise from the same underlying dynamics, differing only in amplitude and persistence. This unification removes the need to invoke fundamentally different mechanisms for excursions and reversals, and is consistent with their shared geometric signatures.

9.6 Relation to Broader Earth-System Models

Although the present analysis is framed in terms of geomagnetic and inertial modes, the results are compatible with broader Earth-system hypotheses involving episodic core–mantle decoupling, rotational instability, and energy redistribution. The geometric and statistical constraints identified here provide testable benchmarks for such models, independent of specific mechanistic details.

Crucially, the analysis does not rely on any single explanatory framework. Instead, it establishes empirical geometric relationships that any successful theory of geomagnetic excursions must reproduce.

In the following section, we discuss limitations, uncertainties, and directions for future work.

10 Limitations, Uncertainties, and Sensitivity

10.1 Data Coverage and Sampling Bias

Despite the large size of the combined GEOMAGIA dataset, data coverage is uneven in both time and space. Sedimentary records dominate older intervals, while archaeomagnetic and volcanic records contribute disproportionately to the late Holocene and historical periods. These differences introduce potential sampling biases that cannot be entirely eliminated.

To mitigate this, we emphasize geometric and statistical measures that are robust to uneven sampling, such as plane fitting, angular variance, and time-binned means. Cross-dataset replication further reduces the likelihood that observed structure arises from a single data type or region.

Nonetheless, intervals of sparse data—particularly beyond ~ 40 ka—necessarily carry larger uncertainty. Results in these intervals should be interpreted qualitatively rather than quantitatively.

10.2 Age Uncertainty and Temporal Resolution

Age uncertainties in paleomagnetic records vary widely and can exceed the duration of some excursions. While the present analysis does not explicitly propagate individual age uncertainties through the geometric calculations, several factors reduce sensitivity to age errors:

- The focus on Earth-fixed geometry rather than precise timing.
- The use of time binning at scales comparable to or larger than typical age uncertainties.
- The emphasis on persistent geometric structure across multiple excursions.

Nevertheless, future work incorporating probabilistic age models could further refine time-resolved coupling estimates.

10.3 Sensitivity to Binning and Filtering Choices

Several steps in the analysis require choices regarding time-bin width, smoothing, and filtering parameters. Sensitivity tests conducted during this study indicate that the existence and orientation of the geomagnetic excursion plane are robust across a wide range of reasonable parameter choices.

However, the visual prominence of plane-mean signals is sensitive to these choices. Overly aggressive filtering can suppress legitimate excursion structure, while insufficient filtering allows high-frequency noise to obscure geometric trends. The approach adopted here—averaging prior to projection and using moderate bin widths—represents a balance between these extremes.

Importantly, the key quantitative results (plane orientation, angular offset, coupling structure) are not dependent on any single parameter setting.

10.4 Model Simplifications

The synthetic two-mode stochastic model used for comparison is intentionally minimal. It abstracts complex core–mantle dynamics into a low-dimensional phase system with weak coupling and noise. While this simplicity is a strength in terms of interpretability, it necessarily omits many physical processes, including:

- Spatially complex core flow patterns.
- Electromagnetic coupling at the core–mantle boundary.
- Feedbacks between magnetic field intensity and flow structure.

The purpose of the model is not to reproduce all features of the geodynamo, but to demonstrate that the observed geometric and statistical features arise naturally in a weakly coupled system. More detailed numerical models may incorporate these constraints as benchmarks rather than direct targets.

10.5 Alternative Interpretations

Although the results strongly support a two-mode coupled interpretation, alternative explanations cannot be entirely ruled out. For example, long-lived mantle heterogeneity could bias geomagnetic behavior through mechanisms not explicitly modeled here. Similarly, unrecognized data artifacts or systematic biases could, in principle, contribute to apparent structure.

However, the convergence of independent lines of evidence—plane stability, null testing, coupling matrices, time-resolved diagnostics, cross-dataset replication, and synthetic modeling—makes purely coincidental explanations increasingly implausible.

In the final section, we summarize the main conclusions and outline avenues for future research.

11 Conclusions and Outlook

11.1 Summary of Key Findings

This study has developed and applied a comprehensive geometric and statistical framework for analyzing geomagnetic excursions, integrating paleomagnetic observations, Earth-fixed reference geometry, and stochastic dynamical modeling. The principal findings are as follows:

1. Geomagnetic excursion trajectories preferentially occupy a stable Earth-fixed plane near $\sim 170°$E, demonstrably distinct from isotropic or axisymmetric expectations.
2. The excursion plane is systematically offset by approximately $41°$ from an inertial reference plane associated with large-scale mantle structure and true polar wander.
3. This offset is robust under bootstrap resampling, null hypothesis testing, and cross-dataset replication, and cannot be readily attributed to sampling artifacts or random variation.
4. Quantitative coupling matrix analysis reveals a hierarchical coupling structure in which the inertial mode mediates apparent correlations between geomagnetic behavior and other Earth-fixed axes.
5. Time-resolved diagnostics show that coupling strength is episodic and intensifies during excursions, consistent with transient loss of phase stability.
6. A minimal stochastic two-mode phase model reproduces the essential statistical and geometric features of the data without invoking deterministic switching or intrinsic periodicity.

Together, these results provide strong evidence that geomagnetic excursions are not arbitrary deviations of a single-mode geodynamo, but structured manifestations of a weakly coupled Earth system.

11.2 Implications for Geomagnetic Theory

The findings presented here challenge interpretations of geomagnetic excursions that rely solely on internal dynamo noise or ad hoc forcing mechanisms. Instead, they support a view in which

excursions arise from noise-activated phase excursions within a coupled system constrained by Earth-fixed geometry.

This perspective unifies excursions and reversals within a single dynamical framework, differing primarily in amplitude and persistence rather than underlying mechanism. It further implies that geomagnetic behavior cannot be fully understood in isolation from inertial, mantle, and rotational dynamics.

11.3 Broader Earth-System Context

The geometric relationships identified in this study resonate with independent evidence for long-lived Earth-fixed structure in mantle heterogeneity, true polar wander, and rotational stability. The persistent alignment between geomagnetic excursion geometry and these features suggests that geomagnetism participates in a broader Earth-system architecture linking core, mantle, and rotation.

While the present analysis does not require any specific core–mantle decoupling mechanism, it provides quantitative constraints that such mechanisms must satisfy. In this sense, the results serve as an empirical bridge between paleomagnetism and models of whole-Earth dynamics.

11.4 Future Directions

Several avenues for future research follow naturally from this work:

- Incorporation of probabilistic age models to refine time-resolved coupling estimates.
- Extension of the analysis to older excursions and reversals as data coverage improves.
- Integration of intensity data to examine coupling between directional and energetic aspects of the field.
- Application of the geometric framework to fully numerical geodynamo simulations.

More broadly, the methods developed here—statistical plane fitting, coupling matrices, and reduced geometric diagnostics—are readily transferable to other problems involving weakly coupled geophysical systems.

11.5 Closing Remarks

Geomagnetic excursions have long resisted simple classification as either noise or signal. By reframing them as structured, probabilistic expressions of a weakly coupled Earth system, this study provides a coherent explanation for their geometry, variability, and recurrence.

The central insight is not that excursions follow a rigid path, but that they explore a constrained geometric manifold shaped by Earth-fixed structure and dynamical coupling. Recognizing and quantifying this constraint opens new pathways for understanding the magnetic history of our planet and its deep interior dynamics.

References

Gubbins, D. (2007). Geomagnetic reversals. *Nature*, *452*, 165–167. https://doi.org/10.1038/nature06800

Valet, J.-P., Meynadier, L., & Guyodo, Y. (2005). Geomagnetic field strength and reversal rate over the past 2 million years. *Nature*, *435*, 802–805. https://doi.org/10.1038/nature03674

Valet, J.-P., Fournier, A., Courtillot, V., & Herrero-Bervera, E. (2012). Dynamical similarity of geomagnetic field reversals. *Nature*, *490*, 89–93. https://doi.org/10.1038/nature11491

Brown, M. C., Korte, M., & Constable, C. G. (2023). The structure of geomagnetic excursions. *Earth and Planetary Science Letters*, *610*, 117987. https://doi.org/10.1016/j.epsl.2023.117987

Donadini, F., Korte, M., & Constable, C. G. (2009). Geomagnetic field for 0–3 ka: 1. New data sets for global modeling. *Geochemistry, Geophysics, Geosystems*, *10*, Q06007. https://doi.org/10.1029/2008GC002295

Korte, M., Constable, C. G., Donadini, F., & Holme, R. (2011). Reconstructing the Holocene geomagnetic field. *Earth and Planetary Science Letters*, *312*, 497–505. https://doi.org/10.1016/j.epsl.2011.10.031

Evans, D. A. D. (2015). True polar wander. *Treatise on Geophysics*, 2nd ed., Vol. 9, 303–331. https://doi.org/10.1016/B978-0-444-53802-4.00163-0

Dziewonski, A. M., Lekic, V., & Romanowicz, B. (2010). Mantle anchor structure: An argument for bottom-up tectonics. *Earth and Planetary Science Letters*, *299*, 69–79. https://doi.org/10.1016/j.epsl.2010.08.013

Kuramoto, Y. (1984). *Chemical Oscillations, Waves, and Turbulence*. Springer, Berlin. https://doi.org/10.1007/978-3-642-69689-3

Kramers, H. A. (1940). Brownian motion in a field of force and the diffusion model of chemical reactions. *Physica*, *7*, 284–304. https://doi.org/10.1016/S0031-8914(40)90098-2

Channell, J. E. T., Singer, B. S., & Jicha, B. R. (2020). Timing of Quaternary geomagnetic reversals and excursions in volcanic and sedimentary archives. *Quaternary Science Reviews*, 228, 106114. https://doi.org/10.1016/j.quascirev.2019.106114

Molina-Cardín, A., Dinis, L., & Osete, M. L. (2021). Simple stochastic model for geomagnetic excursions and reversals reproduces the temporal asymmetry of the axial dipole moment. *Proceedings of the National Academy of Sciences*, 118(10), e2017696118. https://doi.org/10.1073/pnas.2017696118

GFZ German Research Centre for Geosciences. Modelling geomagnetic excursions. Available at: https://www.gfz.de/en/section/geomagnetism/projects/previous-projects/modelling-geomagnetic-excursions

A Data Processing and Coordinate Conventions

All paleomagnetic directions are converted from declination and inclination to unit vectors in an Earth-fixed Cartesian reference frame. Longitudes are expressed east-positive, and all vectors are normalized prior to analysis. Archaeomagnetic and sedimentary datasets are merged after harmonization of age units and filtering for valid directional information.

Time binning is applied only for reduced diagnostics and plane-mean extraction; all plane fitting and null tests are performed on unbinned unit vectors.

B Null Model Construction

Two classes of null models are employed:

1. **Isotropic null**: Directions are randomized uniformly on the sphere.
2. **Axial null**: Directions are randomized subject to axial symmetry about the rotation axis.

Both nulls preserve the number of observations and temporal sampling but destroy Earth-fixed longitudinal structure. Plane fitting and angular separation statistics are recomputed for each null realization.

C Bootstrap and Uncertainty Estimation

Bootstrap resampling is performed by drawing with replacement from the original VGP dataset. For each realization, the best-fit plane normal is computed and its angular deviation from the ensemble mean is recorded. Reported uncertainties correspond to the 68% and 95% confidence intervals of the bootstrap distribution.

D Coupling Matrix and Conditional Covariance

The coupling matrix is constructed from pairwise angular separations and covariances among Earth-fixed reference vectors. Conditional covariance is evaluated by linearly removing the contribution of the inertial mode prior to computing residual covariance, allowing discrimination between direct and mediated coupling.

E Synthetic Two-Mode Model

The synthetic comparison model consists of a stochastic phase variable weakly coupled to a preferred phase offset. Noise-driven excursions arise through Kramers-type escape from a metastable state. Model parameters are chosen to reproduce observed excursion durations and angular variance, rather than tuned to individual events.